Journal of the Indian Institute of Science
A Multidisciplinary Reviews Journal
ISSN: 0970-4140 Coden-JIISAD

REVIEWS

Reconstruction of Two-Dimensional Spectra from One-Dimensional Projections—Examples from Solid State NMR

*Bibhuti B. Das[1] and K.V. Ramanathan[2]**

Abstract | The use of Projection Reconstruction (PR) to obtain two-dimensional (2D) spectra from one-dimensional (1D) data in the solid state is illustrated. The method exploits multiple 1D spectra obtained using magic angle spinning and off-magic angle spinning. The spectra recorded under the influence of scaled heteronuclear scalar and dipolar couplings in the presence of homonuclear dipolar decoupling sequences have been used to reconstruct J/D Resolved 2D-NMR spectra. The use of just two 1D spectra is observed sufficient to reconstruct a J-resolved 2D-spectrum while a Separated Local Field (SLF) 2D-NMR spectrum could be obtained from three 1D spectra. The experimental techniques for recording the 1D spectra and procedure of reconstruction are discussed and the reconstructed results are compared with 2D experiments recorded in traditional methods. The application of the technique has been made to a solid polycrystalline sample and to a uniaxially oriented liquid crystal. Implementation of PR-NMR in solid state provides high-resolution spectra as well as leads to significant reduction in experimental time. The experiments are relatively simple and are devoid of several technical complications involved in performing the 2D experiments.

1 Introduction

Multidimensional (nD) experiments are routinely used in NMR spectroscopy to correlate resonance frequencies of homo and heteronuclei. As a result, high-resolution spectra are acquired, facilitating unambiguous spectral assignment. Hence, they have become indispensable tools for structure and functional studies in molecules ranging from materials, small organic molecules to supramolecular assemblies in proteins. Since the early seventies, with the development of sophisticated experiments with multidimensions, typical 2D, 3D and 4D experiments are being used in protein structure determination, where each dimension carries resonance frequencies either from the same nucleus or from different nuclei.[1–3] However, the experiment time increases with the increase in dimensionality, which limits the high-resolution spectroscopic approaches. Although, electronics and hardware developments for NMR spectroscopy have improved, other issues related to stability of the sample, and performance of Radio Frequency (RF) circuitry etc., are still unavoidable during the duration of multidimensional experiments and in particular solid state NMR applications to biomolecules.[4–8] For example, structural studies of polycrystalline globular proteins and hydrated biological samples such as the case in membrane proteins in their supramolecular assembly require high dimensional experiments. Of late, emphasis is being drawn on structure determination of membrane protein in oriented phospholipid bilayers by static Oriented Sample (OS) and Magic Angle Spinning (MAS) solid state NMR experiments.[9–11] Separated Local Field (SLF) NMR spectroscopy has been widely used

[1]*Department of Chemistry and Biochemistry, University of California, San Diego, California 92093, USA.*
[2]*NMR Research Centre, Indian Institute of Science, Bangalore, India.*
**kvr@nrc.iisc.ernet.in*

in static OS solid state NMR[12–13] to obtain anisotropic chemical shifts and heteronuclear dipolar frequencies as angular restraints for structure calculation. In these types of experiments, ^{1}H, ^{13}C, ^{15}N anisotropic chemical shifts are correlated with the ^{1}H-^{15}N and ^{1}H-^{13}C dipolar couplings in two and three-dimensions. Recently, MAS techniques were developed to correlate anisotropic interactions with isotropic chemical shifts to measure angular restraints in proteoliposome samples.[14–15] MAS solid state NMR experiments have also been applied to globular proteins to measure heteronuclear dipolar couplings in order to measure order parameters at the atomic level.[16] The order parameters are readily translated into structural and dynamics information in proteins.[16] Numerous pulse schemes have been developed for SLF spectroscopy in static[17–21] and MAS solid state NMR.[14–15,22] Besides proteins, SLF techniques are now routinely applied to liquid crystals to study structure, topology, dynamics and phase transitions. Even for liquid crystalline studies, 2D experiments of long duration are required as the samples are heat sensitive, and long delays are required between each scan. The above points are about major drawbacks in the application of multidimensional experiments and require exploration of alternative methods to circumvent these issues. In order to alleviate this problem, several approaches for speeding up the experiments are being investigated both for liquids[23–28] and solids.[29–34] For example, sparse sampling schemes are of particular importance as nDspectra are recorded with reduced number of data points and are able to reduce the acquisition time by an order of magnitude.[35–38] However, higher and higher dimensional experiments are proposed in order to study larger and larger biomolecules. The prime concern however, is speed. The idea behind some of the reduced dimensionality techniques[23] is to vary two or more evolution periods simultaneously and in step with one another. The corresponding signals are detected as sum and difference frequencies. Alternately in the Projection Reconstruction (PR) approach,[39] multidimensional spectra are reconstructed from the projections of a number of lower dimensional spectra. The concept of projection-reconstruction is widely applied in many branches of science, namely Computed Tomography and Magnetic Resonance Imaging. Projection-reconstruction is therefore, a fairly well established approach. Its application to high-resolution NMR spectroscopy is relatively recent. The technique was introduced to solution NMR spectroscopy[40,41] and is also being considered for solid state NMR. In the oriented sample solid state studies, SLF 2D spectrum was reconstructed from few 1D projections.[29]

In this article, we show that PR NMR techniques can be applied to solid samples with simple solid-state NMR experiments. The magic angle spinning and off-magic angle spinning techniques are explored in one dimensional data acquisition. Multiple one-dimensional spectra were recorded encoding chemical shifts and heteronuclear scalar and dipolar frequencies. Heteronuclear couplings were scaled under the influence of homonuclear Radio Frequency (RF) pulses, determining the projection angles for each 1D spectrum. The recorded 1D spectra were then used to reconstruct a two-dimensional spectra. Example of a (2D) J-resolved spectrum from a polycrystalline sample spinning at magic angle reported earlier by us[42] is first discussed. Subsequently, the reconstruction of a 2D-Separated Local Field (SLF) spectrum from one-dimensional spectra under variable angle sample spinning is demonstrated for the first time. The results obtained from partially oriented liquid crystalline samples using the PR NMR are compared with the spectra obtained from conventional 2D NMR experiments.

2 Reconstruction

Realizing the fact that a regular three-dimensional spectrum is a sparse distribution of discrete resonances similar to a 3D object as a physiological sample, PR has been recently applied to high-resolution NMR spectroscopy.[39,41,43–44] Projection-reconstruction relies on the Fourier transform slice/projection theorem to generate a set of projections at different inclinations. Reconstruction is implemented by one of three possible deterministic back-projection scheme (additive, lowest-value, or algebraic), or by a statistical model-fitting program.[40] A few one-dimensional projections of a two-dimensional matrix array, projected along defined angles, are sufficient to recreate the entire matrix. The number of projections required would depend upon the complexity of the spectrum. For example, in a simple 2D heteronuclear J-resolved spectrum, 0° and 90° projections of the spectrum along the $\mathbf{F}_2$ and $\mathbf{F}_1$ dimensions respectively correspond only to chemical shifts and J-couplings, without any correlation between shifts and couplings. On the other hand, a 45° projection, which is equivalent to recording a proton coupled carbon spectrum, provides the required correlation, and together with the $\mathbf{F}_2$ projection may be used to construct the full 2D spectrum. This is illustrated in Figure 1. The pulse scheme is shown in Figure 1A with standard Cross-Polarization (CP) pulses and Composite Pulse Decoupling (CPD) for ^{1}H nuclei. The projection matrix is shown in Figure 1B with

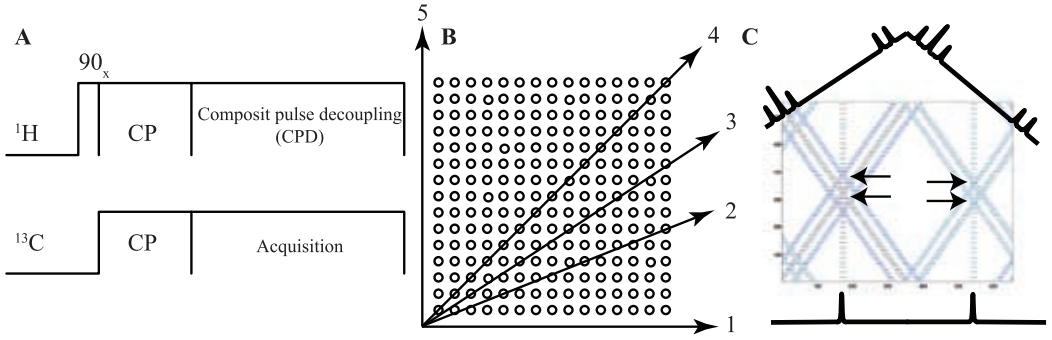

Figure 1: A) pulse scheme used for recording one dimensional data. CP stands for cross-polarization under Hartmann Hahn condition. B) Graphical representation of projection reconstruction technique. Arrows represent the projection angles corresponding to the chemical shift only data and the same with proton coupling. C) Cartoon diagram of the 1D projections and reconstruction. The minimal cross-section points are marked with the arrows for better visualization.

arrows corresponding to the projection angles for 1D data sets. Projections along 1 ($\mathbf{F}_2$) and 5 ($\mathbf{F}_1$) correspond to the 1D data recorded for chemical shifts and heteronuclear J couplings respectively. On the other hand, the projections along 4 represent the ^{1}H coupled 1D spectrum. The proton-coupled spectra with scaled J-couplings define the projections along 2 and 3 respectively.

In the case of solids, 1D data, with only chemical shifts, are acquired under the influence of heteronuclear decoupling pulses. Similarly, shiftless NMR spectroscopy can be applied to obtain heteronuclear dipolar frequencies only.[45] This technique can be used to obtain 1D spectrum encoding J couplings with a simple modification in the pulse scheme shown in Figure 1 in combination with magic angle sample spinning. In order to obtain a spectrum with resolved heteronuclear J couplings, a homonuclear dipolar decoupling sequence along with magic angle spinning needs to be used while acquiring the spectrum. The homonuclear decoupling scales the heteronuclear J coupling interaction, and hence the observed splitting of the carbon peaks are reduced. The obtained 1D spectrum corresponds to a projection of the 2D spectrum with a projection angle less than 45°. The precise angle depends on the homonuclear decoupling sequence used, and may be obtained from experiments on a standard sample in the solid and solution state.

In solids, the scaling factor was estimated by comparing the J-splitting of the proton-coupled carbon spectra of the samples dissolved in suitable organic solvents. The scaling arises from the use of homonuclear dipolar decoupling during acquisition and the scaling factor is given by cos β, where β is the angle between the effective field axis and the z-axis. For the PMLG pulse sequence for which the effective field is along the magic angle $\beta_m = 54.7$, the J coupling Hamiltonian $H_J = JI_ZS_Z \cos \beta_m$. The carbon chemical shift is unaffected by the proton decoupling used during acquisition. For the reconstruction of the 2D J-resolved spectrum from these two 1D spectra, the procedure suggested for reconstructing PISEMA spectra from corresponding 1D spectra has been used.[29] The 1D spectra recorded with different scaling factors cos β, correspond to projections along different axes of the 2D J-resolved spectrum. The projection angle θ of these axes with respect to the chemical shift axis of the 2D spectrum is given by

$$\theta = \arctan(\cos \beta) = \arctan \frac{S_J}{S_{cs}}, \qquad (1)$$

where S_J and S_{CS} are the scaling factors for the J coupling and chemical shift respectively. The 1D data corresponding to different projection angles are included in a 'MATLAB' program to reconstruct the 2D spectrum as follows. The 1D spectrum is stored as the central row of a matrix. It is then mapped to all the other rows, according to the projection angle required, which is achieved by setting the $(i + k, j + 1)$ element of the matrix to be equal to (i, j)th element, such as $\tan \theta = 1/k$. For example, the spectrum with only chemical shift is mapped to all the rows as it is. The matrix corresponding to the J-coupled spectrum is generated by shifting the data points between consecutive rows, so as to create a skewed data set with the required tilt angle given by Equation 1. From the J coupled spectrum two such matrices are created since the positive and negative values of the J couplings are indistinguishable and symmetry is exhibited by the 2D spectrum with respect to the central row. After the construction of the three matrices (A, B, C) mentioned above, they are overlapped to

obtain the final matrix F in which each element is the minimum of the corresponding element of the three overlapped matrices, i.e., $\mathbf{F}_{ij} = \min(\mathbf{A}_{ij}, \mathbf{B}_{ij}, \mathbf{C}_{ij})$. Therefore, only those points in the final matrix are significant where all the three matrices simultaneously have some finite value. The matrix thus obtained represents the 2D spectrum corresponding to a J-resolved experiment.

3 Reconstruction of a Solid-State High-Resolution Heteronuclear J Resolved 2D Spectrum from 1D Experiments

Heteronuclear J-couplings have been exploited in NMR in a number of ways. In the case of liquids, the one-bond couplings have been used as an assignment tool to distinguish primary, secondary, tertiary and quaternary carbons. Heteronuclear polarization transfer techniques such as INEPT[46] have been exploited J-couplings to provide sensitivity enhancement to the insensitive nuclei. Multidimensional heteronuclear correlation experiments provide connectivity information between several sets of nuclei that have J-coupling between them. As one of the ways of editing a complex carbon spectrum and providing assignments, heteronuclear J-resolved spectroscopy is a very useful tool. However, this technique is being used relatively less frequently because of the significantly long time required for the experiment, while 1D experiments like DEPT[47] provide carbon multiplicity information in a much shorter time and are used more widely. Nevertheless, there is a definite advantage with the J-resolved spectroscopy approach as it provides unambiguous identity of the chemical group since the multiplet structure is visible in the 2D spectrum, in contrast to other 1D editing techniques. It is also emerging as a key method in the metabolomics toolbox.[48] In solids, spectral editing is usually done by utilizing dipolar couplings.[49–50] However, the method is not universally applicable as the dipolar couplings show a lot of variability due to local motions. In recent times, the possibility of using J coupling for correlation and spectral editing experiments has been demonstrated.[51–54] The experimental spectra are shown for a plastic crystalline sample of camphor spinning at magic angle. The carbon chemical sites were assigned following the multiple quantum (mQ) filtered spectra with coherence transfer efficiency at 100%, 28%, 6% and 12% for 1Q, 2Q and 3Q filtering experiments respectively.[55–57] The assignment is shown for the molecule in Figure 2A. A total number of 514 scans with 5 second recycle delay were used to acquire the total data points, which correspond to a total of 43 minutes of experiment time. Similarly the J-resolved 2D

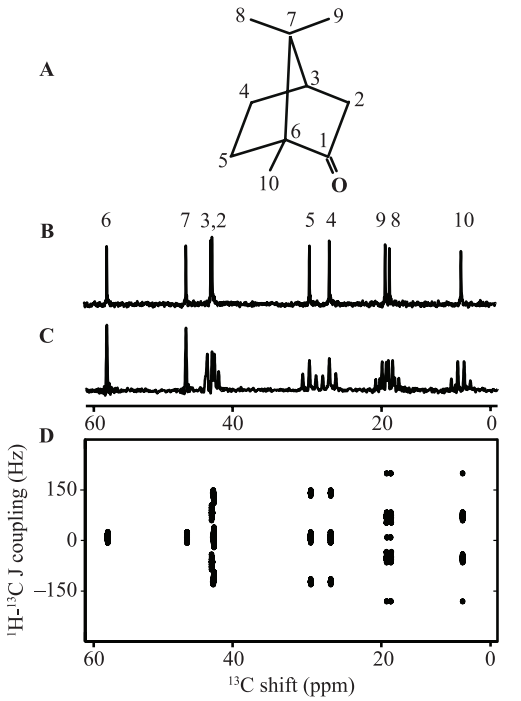

Figure 2: A) Molecular structure of camphor with numbers assigned to carbon nuclei. B) and C) 1D ^{13}C spectra obtained from SPINAL and PMLG-9 decoupling. D) 2D J-resolved spectrum of camphor reconstructed using the 1D data shown in B and C. The spectrum correlates ^{13}C shifts and ^{1}H-^{13}C J couplings in Hz. [Reproduced with Permission from *Chem. Phys. Lett.*, **2007**, 442, 474.]

experiment on camphor was reported by Nielsen et al. using SEMUT pulse technique.[58] SEMUT[59] pulse sequence has been used for spectral editing via scalar coupling multiplets. The 2D spectrum for camphor was recorded with 32 increments for indirect evolution and 15 ms mixing period. However, the method is time consuming and requires extra effort for implementation on the spectrometer, and a long experimental time. Recently, the method for Projection Reconstruction from One-Dimensional Spectra (PRODI) has been proposed for the SLF experiments in static oriented biomolecules.[29] This method has been adapted here for the reconstruction of J-resolved 2D spectra. Heteronuclear J resolved spectrum were reconstructed from ^{13}C one-dimensional spectra of solid samples of camphor spinning at the magic angle. Two different spectra were obtained with different proton decoupling schemes, and it is shown that these two spectra are sufficient to obtain good quality J resolved spectrum of the sample under study.

The experiments reported here were performed on a Bruker DSX-300 NMR spectrometer equipped with a 4 mm MAS probe and working at ^{1}H and ^{13}C resonance frequencies of 300.13 MHz

and 75.47 MHz respectively. The ^{13}C spectra of samples of camphor were recorded. The CPMAS pulse sequence shown in Figure 1 was used for acquiring ^{13}C 1D spectra under two different decoupling schemes, at a spinning rate of 7 kHz. The Composite Pulse Decoupling (CPD) during acquisition uses either SPINAL-64[60] or PMLG9[61] in consecutive experiments. The experiment with SPINAL-64 decoupling shows a ^{1}H decoupled carbon spectrum in Figure 2B. In the second experiment, PMLG9 removes homonuclear dipolar coupling. The heteronuclear dipolar coupling is removed by the magic angle spinning. Hence the spectrum in Figure 2C exhibit ^{13}C chemical shift and scaled heteronuclear J-couplings. In case of camphor, the scaling for the chemical shift frequency is one. The J-coupling is scaled by a factor of 0.57. Hence the 1D spectrum obtained from the PMLG9 decoupling was projected at an angle of 30°. The reconstructed 2D J-resolved spectrum is shown in Figure 2D.

4 Reconstruction of High Resolution SLF 2D Spectrum from 1D Experiments with Variable Angle Sample Spinning

This section of the article demonstrates the extension of the methodology described in the previous section for reconstructing a Separated Local Field (SLF) spectrum under variable angle spinning. In separated local field spectroscopy, the widely used pulse scheme uses ^{1}H-^{1}H homonuclear decoupling pulses with simultaneous spin lock pulses on low gamma nuclei (i.e.[15] N and ^{13}C for this article). When the strength of the RF pulses on both nuclei match under Hartmann-Hahn condition, spin exchange occurs, which is then encoded in an indirect dimension followed by the direct acquisition of chemical shifts under ^{1}H heteronuclear decoupling pulses. Upon Fourier transformation of the time domain data in both dimensions, the SLF-2D spectrum correlates the heteronuclear dipolar coupling frequencies in $\mathbf{F}_1$ axis with its corresponding carbon chemical shift along $\mathbf{F}_2$ axis.

Recently, the projection reconstruction method was shown to be useful in provides high-resolution spectrum that is reconstructed from a series of simple 1D experiments. Bertelsen et al.[29] applied the technique to reconstruct a high-resolution SLF 2D spectrum mimicking the PISEMA[13] spectrum. A variety of homonuclear decoupling pulse sequences with their scaling factors and the translated projection angles are shown to provide an impactful spectrum from a single crystal sample. Additionally, the application of PR NMR in biological samples with the reconstruction of PISA wheel type pattern for an alpha helix was also been discussed. However, the optimal conditions for projection reconstruction techniques may vary depending upon the observable line widths and complexity of the spectrum.

Variable angle spinning provides flexibility in terms of choice of projection angles. Off-magic angle spinning scales dipole-dipole interactions and chemical shift anisotropy as well. The technique requires relatively lower RF power on both the channels for cross-polarization and for proton decoupling during acquisition. The lower RF input is due to the reduction in dipolar interactions, proton and carbon chemical shift dispersions. This may particularly be more effective in high magnetic field application with additional sensitivity and resolution. A major concern of using high RF power leading to sample heating is certainly diminished.

RF heating has an undesirable effect on samples like nematic liquid crystals, which are sensitive towards heating, and also on biological samples with more dielectric contents like salts and other ions. In practice, SLF 2D experiments on liquid crystals are carried out with longer delays between successive scans during signal averaging. Hence, there is a substantial increase in acquisition time. It is also noteworthy that setting up of the 2D SLF experiment is time consuming and tedious, depending upon the type of SLF experiments.

Here we have adapted the same projection reconstruction procedure and applied to the liquid crystal samples. It is observed that ^{1}H coupled 1D carbon spectra are either broad or resulted with poor resolution under homonuclear decoupling pulse schemes. The broadening in the carbon spectrum is due to the fast dephasing of the magnetization in the presence of heteronuclear and homonuclear dipolar couplings in liquid crystals. However, homonuclear dipolar couplings between proton nuclei are reduced to its first order under homonuclear decoupling pulses during acquisition. At the same time heteronuclear dipolar frequencies are also been scaled. The resolution of the spectrum is directly governed by the strength of the scaled dipolar couplings. Irrespective of its reduction in dipolar interaction strength, poor resolution in the reconstructed spectrum was observed. This severely limits the practical application in macromolecules such as proteins and other biological samples.

The complete elimination of heteronuclear dipolar couplings in liquid crystals is however, achieved with Magic Angle Sample Spinning

(MASS). The same MAS technique used for recording J coupled spectrum described earlier is applied to liquid crystals, but in a manner that dipolar couplings are also observed. Liquid crystals often provide high-resolution spectrum as the ^{13}C line widths are greatly reduced under MAS. Low RF power is also required for proton decoupling as the homonuclear dipole-dipole interactions are reduced due to MAS. For the requirement of reconstruction procedure, heteronuclear dipolar couplings need to be reintroduced in such a way that the proton coupled ^{13}C spectrum is well resolved. This can be achieved with Off Magic Angle Spinning (OMAS) of liquid crystals.[62–63] Several NMR studies of liquid crystals that utilize near magic angle spinning have been reported.[64–66] It was shown that liquid crystals, when spun about an axis tilted from B_0 at an angular velocity larger than the critical frequency (ω_c), the director of the uniaxially oriented liquid crystals orient along the spinning axis due to the counter balance between the magnetic and viscous torques.[67–68] The macroscopic orientation of the director is determined depending upon the magnetic susceptibility ($\Delta\chi$) of the liquid crystals.

5 Director Dynamics

When a nematic liquid crystal is kept static in a magnetic field, the potential energy per unit volume due to alignment of the director is given by[68]

$$P = -\frac{1}{6}\Delta\chi H^2(3\cos^2\alpha - 1), \qquad (2)$$

where α is the angle between the director and the magnetic field, H is the magnetic field and $\Delta\chi = \chi_{||} - \chi_{\perp}$ is the anisotropy of the magnetic susceptibility; this potential produces a torque on the liquid crystal whose magnitude per unit volume is given by

$$\tau_m = \Delta\chi H^2 \cos\alpha \sin\alpha \qquad (3)$$

From Equation 3, it is clear that for $\Delta\chi > 0$, the potential energy is minimum when $\alpha = 0°$. Thus the liquid crystals of positive $\Delta\chi$ when placed in a uniform magnetic field, its director homogeneously aligns parallel to the magnetic field as shown in Figure 3C. The alignment occurs at a finite rate due to the presence of viscosity in the liquid crystals. The viscous torque (τ_v) is $\tau_v = \gamma_1\dot{\alpha}$, where $\dot{\alpha}$ is the rate of change of the direction of the director, and γ_1 is the Leslie Twist viscosity coefficient. The type of torques present in the sample balances between them to yield the equation of motion for the angle α.

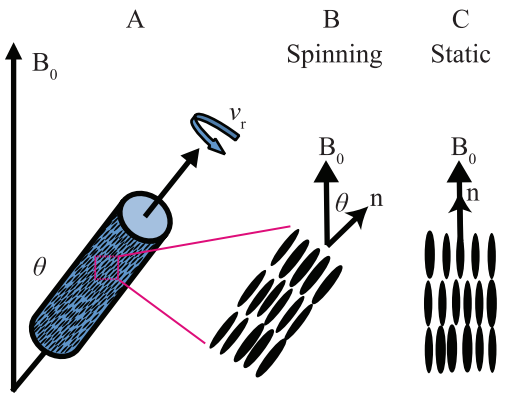

Figure 3: Graphical demonstration of director dynamics in liquid crystals under variable angle sample spinning. A) Rotor filled with liquid crystals undergoing spinning at an arbitrary rotation angle. B) Zoomed in diagram from A with liquid crystal director 'n' pointing along the rotation axis. C) same as in B except that the liquid crystal sample is stationary in the magnetic field with the director 'n' pointing along the magnetic field.

6 Slow Spinning Sample

When the liquid crystal is spun at an angular rate much higher than the critical rate, the director does not have time to orient parallel to the field, but will orient such that the potential energy, described in Equation 2, taken over in one orientation is minimum. The average potential energy is obtained by averaging of $\cos^2\alpha$ over one cycle of the rotation. Considering the reference frame to the orientation of the director characterized by the polar angle γ and an azimuthal angle ϕ, average of $\cos^2\alpha$ can be obtained, and so as the average potential energy. If the magnetic field makes an angle β with the spinning axis, in this frame, the magnetic field vector is described with a constant polar angle β and a constantly changing azimuthal angle $\phi_m = \omega t$ with respect to the director. The cosine of the angle α between the director and the magnetic field is then given as,

$$\cos\alpha = \cos\beta\cos\delta + \sin\beta\sin\delta\cos(\varphi_m - \varphi_n) \qquad (4)$$

and the average over one cycle is given as

$$\cos^2\alpha = \cos^2\beta\cos^2\delta + (1/2)\sin^2\beta\sin^2\delta \qquad (5)$$

Inserting Equation 5 into Equation 2, the average potential is given as,

$$P = -(1/3)\Delta\chi H^2[(3\cos^2\beta - 1)/2][(3\cos^2\delta - 1)/2] \qquad (6)$$

From Equation 6, it follows that for liquid crystals of positive $\Delta\chi$ and $\beta < \theta_m$, the director aligns

along the spinning axis as shown in Figure 3B. When $\beta = \theta_m$ there is no orientation effect, and when $\beta > \theta_m$ the director distributes in the plane perpendicular to the spinning axis. It is just the reverse in case of liquid crystals with negative $\Delta\chi$.

Under static condition, a proton coupled carbon has resonance frequencies given by

$$\omega \pm = \omega_0(1 - \sigma_{zz}) \pm (J + 2D_{zz})/2, \quad (7)$$

where J is the isotropic scalar coupling, σ_{zz} and D_{zz} are the chemical shift and the dipolar coupling in the laboratory frame. In the molecular frame, σ_{zz} and D_{zz} are given by,

$$\sigma_{zz} = \sigma_{iso} + (2/3)\Delta\sigma S(3\cos^2\alpha - 1)/2 \quad (8)$$

$$D_{zz} = SD_{33}(3\cos^2\alpha - 1)/2, \quad (9)$$

where S is the order parameter of the molecule, α is the angle between the director, and the local z-axis, D_{33} is the dipolar-coupling constant between the carbon and proton, $\Delta\sigma$ is the chemical shift anisotropy and σ_{iso} is the isotropic chemical shift.

When the liquid crystalline sample is spun at some spin rate above the critical rate, α becomes time dependent and can be written as

$$\begin{aligned}(3\cos^2\alpha(t) - 1)/2 = {} & (1/4)(3\cos^2\beta - 1)(3\cos^2\delta - 1) \\ & + (3/4)\sin^2\beta\sin^2\delta\cos(\omega_r t + \varphi) \\ & + (3/4)\sin^2(\beta)\sin^2(\delta)\cos^2(\omega_r t + \varphi),\end{aligned} \quad (10)$$

where β is the angle between the spinning axis and the magnetic field, and δ is the angle between the director and the spinning axis. φ is the initial phase at $t = 0$ and can be considered as $\varphi = 0$. ω_r is the spinning frequency. Hence, the splitting in the doublet of carbon spectrum is given by

$$\Delta\omega = J + S_{33}D_{33}(3\cos^2\beta - 1)(3\cos^2\delta - 1)/2 \quad (11)$$

7 Projection Reconstruction of SLF 2D Spectrum

For the reconstruction of 2D spectrum, 1D data sets were acquired similar to the J coupled spectroscopy, one with heteronuclear decoupling and the others with homonuclear dipolar decoupling on a Bruker DSX 300 NMR spectrometer equipped with a variable angle DOTY probe.[69] The spectra are shown in Figure 4 for a liquid crystal sample of ZLI-1132. Three 1D data sets were recorded, one with SPINAL-64 and the other two were recorded with PMLG-9 and BLEW-48 decoupling. The spectrum shown in Figure 4D corresponds to the carbon

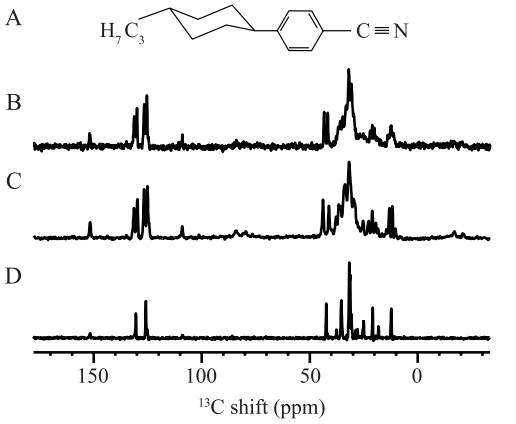

Figure 4: Carbon spectrum of ZLI-1132 obtained with different decoupling pulse sequences. A) Molecular structure of ZLI-1132. B) Spectrum obtained with SPINAL-64 decoupling acquired with 16 scans. C) and D) Spectra obtained with PMLG-9 and BLEW-48 decoupling for 64 scans each. A 5 second recycle delay was used between the successive scans.

chemical shifts of ZLI-1132 liquid crystal obtained under 1500 Hz spinning speed at an angle ~53°. Figure 4B and 4C represent proton coupled carbon spectrum of the same molecules acquired under PMLG-9 and BLEW-48 decoupling respectively.

The 1D data sets were then utilized in the reconstruction procedure. The three 2D matrices reconstructed from 1D spectra were then projected at the angles of 0° for (SPINAL-64), 27° for PMLG-9 and 22° for BLEW-48 decoupled data sets. Here, the projection angles were determined according to the scaling factors associated with the respective pulse schemes. The scaling factors were calculated for the spectrometer with a standard sample and were measured to be 0, 0.5 and 0.4 for SPINAL, PMLG-9 and BLEW-48 pulse sequences respectively. From these 1D spectra three 2D matrices were created as per the procedure described earlier. The three matrices were then overlapped and the minimum of the three matrices provides the 2D-reconstructed spectrum shown in Figure 5.

Figure 5A is the reconstructed spectrum. Figure 5B is the spectrum recorded using the conventional SLF-2D experiment shown for comparison. The spectrum was recorded with BLEW-48 homonuclear decoupling pulse sequence during t_1 evolution. 32 scan for each t_1 increment were used, and a total of 128 t_1 data points were collected before the Fourier transform along the indirect dimension. The recycle delay of 10 second was used to avoid sample heating. 30 kHz RF was used for heteronuclear decoupling pulses and 60 kHz RF was used for homonuclear decoupling in the 2D pulse sequence.

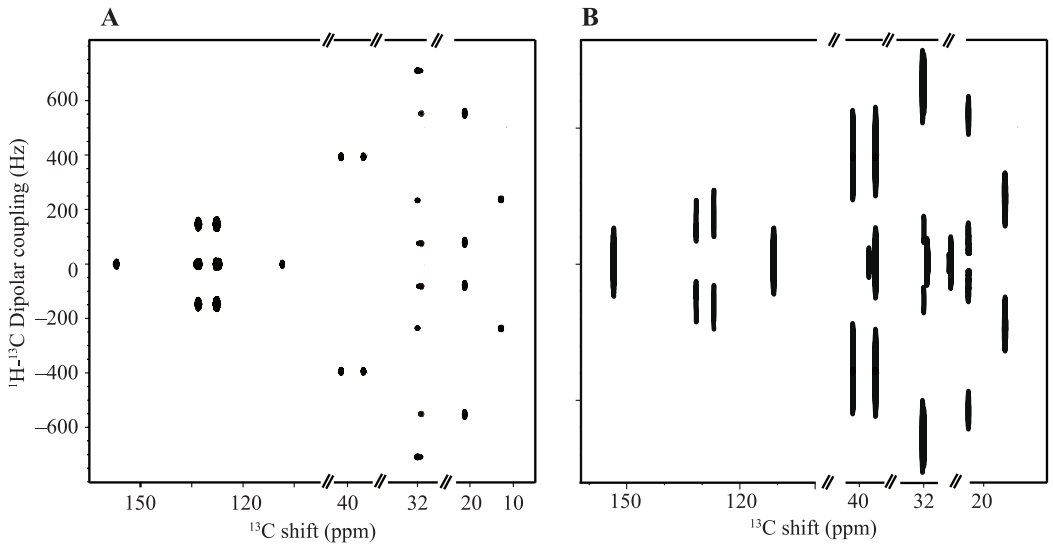

Figure 5: A) Reconstructed 2D SLF spectrum of ZLI-1132. B) 2D VASS-SLF spectrum obtained under the sample spinning at an angle ~53°. The spinning speed was maintained at 1500 ± 2 Hz throughout the experiment. A total of 128 t_1 data points for an evolution period of 12.3 ms was obtained. 30 kHz RF was used for 40 ms decoupling period while acquiring carbon signal. A recycle delay of 10 second between each scan was used during the entire experiment resulting in a total acquisition period of 11.6 hours.

8 Results and Discussion

From the 1D carbon spectrum of camphor in solution NMR, the J-couplings corresponding to CH, CH_2 and CH_3 groups were obtained as 142, 133 and 125 Hz respectively. In the solid state MAS spectra these couplings are scaled to 73, 67 and 64 Hz respectively as seen in Figure 2. After the reconstruction, the J values obtained from the reconstructed spectrum shown in Figure 2 correspond to the unscaled values obtained in solution NMR. The other notable features of the reconstructed spectrum are as follows: The spacing between the spectral lines of carbon 2 and 3 is very small and in the J coupled spectrum, the lines are severely overlapped making it difficult to ascertain the multiplicity of the peaks. These lines are clearly resolved in the reconstructed J-resolved spectrum. Similarly, the overlapped quartet structure corresponding to the carbons 8 and 9 is clearly resolved in the reconstructed spectrum. It may be noted that the spectra of camphor were obtained with just 2 scans for the fully decoupled spectrum and with 16 scans for the J-coupled spectrum with a recycle delay of 5 seconds between scans. A comparison of this with a regular heteronuclear J resolved spectrum in terms of saving of experimental time may be made as follows—Since ^{1}H-^{13}C J couplings may require a window of 600 Hz, and assuming a required line width of 10 Hz in the F_1 dimension, approximately 100 t_1 increments, each with a single transient, would be required for a 2D J-resolved spectrum for sample like camphor. This indicates a saving of time of approximately a factor of three. But more significantly, carrying out a J-resolved spectroscopy experiment in solids is more tedious. The experiment requires that all the pulses are rotor synchronized with the 180° refocusing pulses applied in the middle of the t_1 period.[58] Correspondingly, the t_1 increment has also to be adjusted, not only with sample rotation but also with the cycle time of the homonuclear decoupling sequence used. On the other hand, recording of the 1D spectra is devoid of these problems and is measured using simple and standard cross-polarization pulse schemes available on almost all spectrometers. These experiments are robust and are carried out at various spinning speeds without any rotor synchronization. The reconstructed spectrum in Figure 2D provides a high-resolution spectrum with significant reduction in acquisition time with respect to the traditional method.

The reconstructed 2D SLF spectrum of the liquid crystal ZLI-1132 obtained from using the 1-dimensional VASS spectra (Figure 4) incorporated into a reconstruction algorithm is shown in Figure 5. The reconstructed spectrum is the result of three data sets involved in the reconstruction procedure. Three 1D-experiments, namely one with proton decoupled chemical shift spectrum and the proton-coupled spectra obtained with homonuclear dipolar decoupling pulses are sufficient to reconstruct the 2D spectrum. The

expanded regions of the reconstructed spectrum are shown at different contour levels. Notably few artifacts near zero frequency were observed for aromatic carbons, which could potentially be removed with more projections. However, the overall quality of the spectrum seems to be superior, and multiplet splitting is comparable with the two-dimensional spectrum obtained from VASS-SLF experiments. A total of 11.6 hours of acquisition time was used to acquire the 2D spectrum. As seen from the figures, it is clear that the reconstructed spectrum provides higher resolution. From the splitting of the dipolar frequencies, multiple spin systems are readily identified. For example non-protonated carbons near 110 and 155 ppm show no splitting. Two, three and four dipolar splitting correspond to the CH, CH_2 and CH_3 groups. The additional feature is that the 1D experiments used in the reconstruction process were obtained within a total experimental time of 12 minutes. Hence the method provides a 55-fold reduction in the experiment time compared to the 2D experiment.

9 Summary

It is observed that a heteronuclear 2D J-resolved spectrum of solid samples can be reconstructed from 1D experiments by projecting them on to a 2D plane. Such reconstructed spectra are of good quality with high resolution to resolve overlapped multiple resonances in the 1D spectra. In addition to saving experimental time, the method has certain advantages for solid samples, where setting up the 2D experiment requires very careful adjustments in view of the simultaneous application of magic angle spinning and multiple pulse decoupling. The method has been demonstrated on samples of camphor. Further, high resolution 2D SLF-spectrum was reconstructed using three 1D data sets obtained under SPINAL-64 heteronuclear decoupling pulse scheme, PMLG-9, and BLEW-48 homonuclear dipolar decoupling pulse schemes. The technique of variable angle sample spinning has been used to reduce the homonuclear dipolar couplings among the protons. As a result low power RF is applied to observe high-resolution spectrum with lesser sample heating. This provides an opportunity to study of the liquid crystals with high precisions. VASS also provides flexibility in terms of scaling factor and spectral appearance, which are helpful in generating accurate 2D spectrum. Thus, the reconstruction procedure along with VASS technique provides a tool for an alternative towards 2D experiments in terms of fast data acquisition. The technique offers an opportunity to explore ideas in the process of reconstruction of higher dimensional spectrum in solid state from one and two-dimensional data sets.

Received 9 July 2014.

References

1. Bax, A. Multidimensional nuclear magnetic resonance methods for protein studies. *Current Opinion in Structural Biology* **1994**, *4* (5), 738–744.
2. Schmidt-Rohr, K.; Spiess, H.W. *Multidimensional solid-state NMR and polymers*. Elsevier: **1994**.
3. Bax, A.; Grzesiek, S. Methodological advances in protein NMR. *Accounts of Chemical Research* **1993**, *26* (4), 131–138.
4. Grant, C.V.; Sit, S.L.; De Angelis, A.A.; Khuong, K.S.; Wu, C.H.; Plesniak, L.A.; Opella, S.J. An efficient (1)H/(31)P double-resonance solid-state NMR probe that utilizes a scroll coil. *Journal of Magnetic Resonance* **2007**, *188* (2), 279–284.
5. Grant, C.V.; Wu, C.H.; Opella, S.J. Probes for high field solid-state NMR of lossy biological samples. *Journal of Magnetic Resonance* **2010**, *204* (2), 180–188.
6. Grant, C.V.; Yang, Y.; Glibowicka, M.; Wu, C.H.; Park, S.H.; Deber, C.M.; Opella, S.J. A Modified Alderman-Grant Coil makes possible an efficient cross-coil probe for high field solid-state NMR of lossy biological samples. *Journal of Magnetic Resonance* **2009**, *201* (1), 87–92.
7. Gor'kov, P.L.; Chekmenev, E.Y.; Fu, R.; Hu, J.; Cross, T.A.; Cotten, M.; Brey, W.W. A large volume flat coil probe for oriented membrane proteins. *Journal of Magnetic Resonance* **2006**, *181* (1), 9–20.
8. Stringer, J.A.; Bronnimann, C.E.; Mullen, C.G.; Zhou, D.H.; Stellfox, S.A.; Li, Y.; Williams, E.H.; Rienstra, C.M. Reduction of RF-induced sample heating with a scroll coil resonator structure for solid-state NMR probes. *Journal of Magnetic Resonance* **2005**, *173* (1), 40–48.
9. Opella, S.J. NMR and membrane proteins. *Nat Struct Biol* **1997**, *4 Suppl*, 845–848.
10. Opella, S.J. Structure Determination of Membrane Proteins by Nuclear Magnetic Resonance Spectroscopy. *Annual Review of Analytical Chemistry* **2013**, *6*(1), 305–328.
11. Marassi, F.M.; Das, B.B.; Lu, G.J.; Nothnagel, H.J.; Park, S.H.; Son, W.S.; Tian, Y.; Opella, S.J. Structure determination of membrane proteins in five easy pieces. *Methods* **2011**, *55* (4), 363–369.
12. Hester, R.; Ackerman, J.; Neff, B.; Waugh, J. Separated local field spectra in NMR: determination of structure of solids. *Physical Review Letters* **1976**, *36* (18), 1081.
13. Wu, C.; Ramamoorthy, A.; Opella, S. High-resolution heteronuclear dipolar solid-state NMR spectroscopy. *Journal of Magnetic Resonance, Series A* **1994**, *109* (2), 270–272.
14. Das, B.B.; Nothnagel, H.J.; Lu, G.J.; Son, W.S.; Tian, Y.; Marassi, F.M.; Opella, S.J. Structure determination of a

membrane protein in proteoliposomes. *Journal of the American Chemical Society* **2012**, *134* (4), 2047–2056.

15. Das, B.B.; Zhang, H.; Opella, S.J. Dipolar assisted asignment protocol (DAAP) for MAS sold-state NMR of rotationally aligned membrane proteins in phospholipid bilayers. *J Magn Reson* **2014**, *242*, 224–232.
16. McDermott, A. Structure and dynamics of membrane proteins by magic angle spinning solid-state NMR. *Annu Rev Biophys* **2009**, *38*, 385–403.
17. Lobo, N.P.; Ramanathan, K. Combining adiabatic and Hartmann, ÄìHahn cross-polarization for sensitivity enhancement in solid state separated local field 2D-NMR experiments of partially ordered systems. *Chemical Physics Letters* **2012**, *536*, 155–161.
18. Lobo, N.P.; Ramanathan, K.V. Sensitivity Enhancement in Solid-State Separated Local Field NMR Experiment by the Use of Adiabatic Cross-Polarization. *The Journal of Physical Chemistry Letters* **2011**, *2* (10), 1183–1188.
19. Das, B.B.; Sinha, N.; Ramanathan, K.V. The utility of phase alternated pulses for the measurement of dipolar couplings in 2D-SLF experiments. *Journal of Magnetic Resonance* **2008**, *194* (2), 237–244.
20. Das, B.B.; Ajithkumar, T.G.; Ramanathan, K.V. Improved pulse schemes for separated local field spectroscopy for static and spinning samples. *Solid State Nucl Magn Reson* **2008**, *33* (3), 57–63.
21. Nevzorov, A.A.; Opella, S.J. A 'magic sandwich' pulse sequence with reduced offset dependence for high-resolution separated local field spectroscopy. *Journal of Magnetic Resonance* **2003**, *164* (1), 182–186.
22. Dvinskikh, S.V.; Zimmermann, H.; Maliniak, A.; Sandstrom, D. Heteronuclear dipolar recoupling in liquid crystals and solids by PISEMA-type pulse sequences. *Journal of Magnetic Resonance* **2003**, *164* (1), 165–170.
23. Szyperski, T.; Wider, G.; Bushweller, J.; Wüthrich, K. Reduced dimensionality in triple-resonance NMR experiments. *Journal of the American Chemical Society* **1993**, *115* (20), 9307–9308.
24. Szyperski, T.; Yeh, D.C.; Sukumaran, D.K.; Moseley, H.N.; Montelione, G.T. Reduced-dimensionality NMR spectroscopy for high-throughput protein resonance assignment. *Proceedings of the National Academy of Sciences* **2002**, *99* (12), 8009–8014.
25. Kim, S.; Szyperski, T. *J. Am. Chem. Soc.* **2003**,*125*, 1385.
26. Szyperski, T.; Yeh, D.C.; Sukumaran, D.K.; Moseley, H.N.B.; Montelione, G.T. *Proc. Natl. Acad. Sci. USA.* **2002**, *99*, 8009.
27. Frydman, L.; Scherf, T.; Lupulescu, A. The acquisition of multidimensional NMR spectra within a single scan. *Proceedings of the National Academy of Sciences* **2002**, *99* (25), 15858–15862.
28. Mishkovsky, M.; Frydman, L. Principles and progress in ultrafast multidimensional nuclear magnetic resonance. *Annual review of physical chemistry* **2009**, *60*, 429–448.
29. Bertelsen, K.; Pedersen, J.M.; Nielsen, N.C.; Vosegaard, T. 2D separated-local-field spectra from projections of 1D experiments. *Journal of Magnetic Resonance* **2007**, *184* (2), 330–336.
30. Brüschweiler, R.; Zhang, F. Covariance nuclear magnetic resonance spectroscopy. *The Journal of chemical physics* **2004**, *120* (11), 5253–5260.
31. Astrof, N.S.; Lyon, C.E.; Griffin, R.G. Triple resonance solid state NMR experiments with reduced dimensionality evolution periods. *Journal of Magnetic Resonance* **2001**, *152* (2), 303–307.
32. Atreya, H.S.; Szyperski, T. G-matrix Fourier transform NMR spectroscopy for complete protein resonance assignment. *Proceedings of the National Academy of Sciences of the United States of America* **2004**, *101* (26), 9642–9647.
33. Szyperski, T.; Atreya, H.S. Principles and applications of GFT projection NMR spectroscopy. *Magnetic Resonance in Chemistry* **2006**, *44* (S1), S51–S60.
34. Franks, W.T.; Atreya, H.S.; Szyperski, T.; Rienstra, C.M. GFT projection NMR spectroscopy for proteins in the solid state. *J Biomol NMR* **2010**, *48* (4), 213–223.
35. Atreya, H.S.; Szyperski, T. Rapid NMR data collection. *Methods in enzymology* **2005**, *394*, 78–108.
36. Hyberts, S.G.; Arthanari, H.; Robson, S.A.; Wagner, G. Perspectives in magnetic resonance: NMR in the post-FFT era. *Journal of Magnetic Resonance* **2014**, *241* (0), 60–73.
37. Rovnyak, D.; Frueh, D.P.; Sastry, M.; Sun, Z.-Y.J.; Stern, A.S.; Hoch, J.C.; Wagner, G. Accelerated acquisition of high resolution triple-resonance spectra using non-uniform sampling and maximum entropy reconstruction. *Journal of Magnetic Resonance* **2004**, *170* (1), 15–21.
38. Jaravine, V.; Ibraghimov, I.; Orekhov, V.Y. Removal of a time barrier for high-resolution multidimensional NMR spectroscopy. *Nature methods* **2006**, *3* (8), 605–607.
39. Kupče, Ē.; Freeman, R. Projection–Reconstruction Technique for Speeding up Multidimensional NMR Spectroscopy. *Journal of the American Chemical Society* **2004**, *126* (20), 6429–6440.
40. Kupče, E.; Freeman, R. The radon transform: A new scheme for fast multidimensional NMR. *Concepts in Magnetic Resonance Part A* **2004**, *22 A* (1), 4–11.
41. Kupče, E.; Freeman, R. Reconstruction of the three-dimensional NMR spectrum of a protein from a set of plane projections. *J Biomol NMR* **2003**, *27* (4), 383–387.
42. Das, B.B.; Mitra, A.; Ramanathan, K. Reconstruction of a solid-state high-resolution heteronuclear J-resolved 2D spectrum from 1D experiments. *Chemical physics letters* **2007**, *442* (4), 474–477.
43. Kupče, E.; Freeman, R. Fast reconstruction of four-dimensional NMR spectra from plane projections. *J Biomol NMR* **2004**, *28* (4), 391–395.
44. Venters, R.A.; Coggins, B.E.; Kojetin, D.; Cavanagh, J.; Zhou, P. (4, 2) D Projection-Reconstruction Experiments for Protein Backbone Assignment: Application to Human Carbonic Anhydrase II and Calbindin D28K. *Journal of the American Chemical Society* **2005**, *127* (24), 8785–8795.

45. Wu, C.H.; Opella, S.J. Shiftless nuclear magnetic resonance spectroscopy. *The Journal of chemical physics* **2008**, *128* (5), 052312.
46. Morris, G.A.; Freeman, R. Enhancement of nuclear magnetic resonance signals by polarization transfer. *Journal of the American Chemical Society* **1979**, *101* (3), 760–762.
47. Pegg, D.T.; Bendall, M.R. Two-dimensional DEPT NMR spectroscopy. *Journal of Magnetic Resonance (1969)* **1983**, *55* (1), 114–127.
48. Ludwig, C.; Viant, M.R. Two-dimensional J-resolved NMR spectroscopy: Review of a key methodology in the metabolomics toolbox. *Phytochemical Analysis* **2010**, *21* (1), 22–32.
49. Wu, X.L.; Burns, S.T.; Zilm, K.W. Spectral Editing in CPMAS NMR. Generating Subspectra Based on Proton Multiplicities. *Journal of Magnetic Resonance, Series A* **1994**, *111* (1), 29–36.
50. Sangill, R.; Rastrupandersen, N.; Bildsoe, H.; Jakobsen, H.J.; Nielsen, N.C. Optimized Spectral Editing of 13C MAS NMR Spectra of Rigid Solids Using Cross-Polarization Methods. *Journal of Magnetic Resonance, Series A* **1994**, *107* (1), 67–78.
51. Lesage, A.; Bardet, M.; Emsley, L. Through-bond carbon-carbon connectivities in disordered solids by NMR. *Journal of the American Chemical Society* **1999**, *121* (47), 10987–10993.
52. Lesage, A.; Emsley, L. Through-bond heteronuclear single-quantum correlation spectroscopy in solid-state NMR, and comparison to other through-bond and through-space experiments. *Journal of Magnetic Resonance* **2001**, *148* (2), 449–454.
53. Lesage, A.; Sakellariou, D.; Steuernagel, S.; Emsley, L. Carbon-proton chemical shift correlation in solid-state NMR by through-bond multiple-quantum spectroscopy. *Journal of the American Chemical Society* **1998**, *120* (50), 13194–13201.
54. Jayasubba Reddy, Y.; Agarwal, V.; Lesage, A.; Emsley, L.; Ramanathan, K.V. Heteronuclear proton double quantum-carbon single quantum scalar correlation in solids. *Journal of Magnetic Resonance* **2014**, *245* (0), 31–37.
55. Sakellariou, D.; Lesage, A.; Emsley, L. Spectral editing in solid-state NMR using scalar multiple quantum filters. *Journal of Magnetic Resonance* **2001**, *151* (1), 40–47.
56. Elena, B.; Lesage, A.; Steuernagel, S.; Böckmann, A.; Emsley, L. Proton to carbon-13 INEPT in solid-state NMR spectroscopy. *Journal of the American Chemical Society* **2005**, *127* (49), 17296–17302.
57. Lesage, A.; Steuernagel, S.; Emsley, L. Carbon-13 spectral editing in solid-state NMR using heteronuclear scalar couplings. *Journal of the American Chemical Society* **1998**, *120* (28), 7095–7100.
58. Nielsen, N.; Bildsøe, H.; Jakobsen, H.J.; Sørensen, O. Two-dimensional pulse techniques for determination of radio-frequency field strengths and proton multiplicities in NMR spectroscopy. *Journal of the American Chemical Society* **1987**, *109* (3), 901–902.
59. Bildsøe, H.; Dønstrup, S.; Jakobsen, H.J.; Sørensen, O.W. Subspectral editing using a multiple quantum trap: Analysis of J cross-talk. *Journal of Magnetic Resonance (1969)* **1983**, *53* (1), 154–162.
60. Fung, B.; Khitrin, A.; Ermolaev, K. An improved broadband decoupling sequence for liquid crystals and solids. *Journal of Magnetic Resonance* **2000**, *142* (1), 97–101.
61. Vinogradov, E.; Madhu, P.K.; Vega, S. High-resolution proton solid-state NMR spectroscopy by phase-modulated Lee–Goldburg experiment. *Chemical Physics Letters* **1999**, *314* (5–6), 443–450.
62. Poon, C.D.; Fung, B.M. Carbon-13 nuclear magnetic resonance of ferroelectric liquid crystals with off-magic-angle spinning. *The Journal of Chemical Physics* **1989**, *91* (12), 7392–7398.
63. Fung, B.M.; Afzal, J.; Foss, T.L.; Chau, M.H. Nematic ordering of 4-n-alkyl-4-cyanobiphenyls studied by carbon-13 NMR with off-magic-angle spinning. *The Journal of Chemical Physics* **1986**, *85* (9), 4808–4814.
64. Snyder, L.C. Analysis of Nuclear Magnetic Resonance Spectra of Molecules in Liquid-Crystal Solvents. *The Journal of Chemical Physics* **1965**, *43* (11), 4041–4050.
65. Kumar, A.; Suryaprakash, N.; Ramanathan, K.; Khetrapal, C. 'Near magic angle' sample spinning in NMR spectra of molecules oriented in individual and mixed liquid crystals of opposite diamagnetic anisotropies. *Chemical physics letters* **1987**, *136* (2), 227–230.
66. Fung, B.M.; Afzal, J. Carbon-13 NMR of liquid crystals. Spinning near the magic angle with proton-proton dipolar decoupling. *Journal of the American Chemical Society* **1986**, *108* (5), 1107–1108.
67. Courtieu, J.; Bayle, J. P.; Fung, B. M. Variable angle sample spinning NMR in liquid crystals. *Progress in Nuclear Magnetic Resonance Spectroscopy* **1994**, *26, Part 2* (0), 141–169.
68. Courtieu, J.; Alderman, D.; Grant, D.M.; Bayles, J. Director dynamics and NMR applications of nematic liquid crystals spinning at various angles from the magnetic field. *The Journal of Chemical Physics* **1982**, *77* (2), 723–730.
69. Das, B.B.; Separated local field NMR spectroscopy in partially ordered systems—New methodologies and applications, Thesis, Indian Institute of Science, Bangalore, 2008, 103–115.

Bibhuti B. Das 1981. M.Sc. (2003) in Physics from Utkal University, Bhubaneswar and Ph.D. (2008) from Indian Institute of Science, Bangalore, Postdoctoral Fellow at University of California, San Diego, California, USA (2008–2013). Currently at University of California, San Diego as Project Scientist. Co-authored approximately 20 peer review publications. Current research interests are in solid-state nuclear magnetic resonance methods development and applications to biomolecules in their supramolecular assembly.

K.V. Ramanathan received his Ph.D. degree in Physics in 1978 from the Indian Institute of Science, Bangalore for his work on the development of the high pressure-low temperature NMR technique and the study of tunneling and ammonium ion dynamics in solids. In 1977 he joined the Bangalore NMR Facility which eventually became a part of the Indian Institute of Science and switched to working on liquid state NMR and the development of two-dimensional NMR techniques. Subsequently he also became interested in the application of the high-resolution solid state NMR methodologies and in the study of oriented systems and liquid crystals. His other interests include the study of quadrupolar nuclei and overtone spectroscopy and NMR applications to biological systems. Ramanathan has held various positions at the Indian Institute of Science. Currently he is a Professor and the Convener of the SAIF Progamme of DST at IISc. He is a Fellow of the National Academy of Sciences, India and a past President of the National Magnetic Resonance Society.